DOI: 10.1002/cphc.200600659

Ab Initio Study of Poly(vinyl chloride) Propagation Kinetics: Head-to-Head versus Head-to-Tail Additions

Karen Van Cauter, Veronique Van Speybroeck,* and Michel Waroquier[a]

The relative importance of head-to-head versus head-to-tail additions during the free-radical polymerization of vinyl chloride is determined by ab initio methods for different chain lengths of the polymer. First, a level of theory study is performed to determine cost-effective methods for the ab initio description of the propagation kinetics of vinyl chloride. The study includes the following DFT-based methods: B3LYP, B3PW91, BHandH, BHandHLYP, BLYP, BP86, MPW1K and MPW1PW91, in combination with double or triple zeta basis sets 6-31G(d) and 6-311G(d,p). Also, the more recently developed BMK and MPW1K functionals are included. The influence of diffuse functions is tested by comparison with the basis sets 6-31+G(d) and 6-311++G(3df,2p). The best-performing methods are B3LYP, B3PW91 and MPW1K combined with the 6-31+G(d) basis set. The converged probability of head-to-head propagation (2 per 1000 monomer units) is put into relation with the experimental concentrations of defect structures. A comparison is made with the head-to-head (HH) content of fluorine-substituted polymers and poly(vinyl acetate). The ab initio calculations correctly predict the relative sequence of HH content among the various polymers.

1. Introduction

Poly(vinyl chloride) (PVC) is the second most produced plastic in the world (>30 Mton per year), placing after polyolefins and before styrene polymers.[1] The industrial production proceeds mainly via the heterogeneous process of suspension polymerization. A typical PVC molecule contains approximately 1000 vinyl chloride monomer units. The free-radical polymerization mechanism consists of initiation, propagation, chain transfer to small molecules and termination. The propagation step is an important elementary reaction that affects the molecular weight and structural defects of the formed polymer. The vinyl chloride can add to the polymer chain in two ways: head-to-head (HH) or head-to-tail (HT). The general nomenclature is that the "head" of the monomer refers to the more substituted end, while the "tail" of the monomer refers to the less substituted end. Polymer characterization studies show that PVC grows mainly by head-to-tail addition. However, the existence of a small number of head-to-head structures in PVC has been suggested earlier.[2] Structural defects such as head-to-head (HH) units, tertiary chlorines at branched carbons, allylic chlorines (adjacent to internal unsaturations), oxygen containing groups, end groups, and so forth are of practical importance, since they affect the color, thermal stability, crystallinity, processing and mechanical properties of the end products.[3] Especially the susceptibility of PVC synthesized by radical polymerization towards thermal degradation is a point of interest, since the thermal instability of PVC is far more pronounced than that of other important thermoplastics such as polystyrene and poly(methyl methacrylate). This problem is circumvented by adding thermal stabilizers during polymerization. These, however, have a strong negative influence on the environment due to the presence of heavy metals. Further insights into the formation of the defect structures is thus desirable, with the final aim of suggesting alternative ways of stabilizing PVC. The labile defect structures have been extensively searched for by both chemical and spectroscopic methods. Nowadays it is believed that tertiary chlorine and internal allylic chlorine are the most important labile defects in PVC. The former structure is associated with the butyl and a majority of the long chain branches.[4–7]

In this paper, we focus on the relative importance of head-to-head additions in the PVC propagation mechanism. This aspect is of minor relevance for the formation of internal HH linkages, but very important for the formation of short chain (methyl and ethyl) branches and typical end-group structures, as we will discuss further on. It is also closely related to the mechanism of chain transfer to monomer, which plays a very important role in controlling the molecular weight development of PVC polymerization.[2] The reactions that may follow a head-to-head addition are schematically represented in Scheme 1.

The most obvious reaction after a HH addition would seem to be the further propagation of the formed radical by means of a tail-to-tail (TT) addition. In this particular case the HH structure is captured in the PVC molecule, giving rise to an **internal HH linkage**. However, the chlorine atom attached to the second carbon atom in the formed radical can also migrate to the first carbon atom, forming a more stable secondary radi-

[a] *K. Van Cauter, Dr. V. Van Speybroeck, Prof. Dr. M. Waroquier*
Center for Molecular Modeling, Ghent University
Proeftuinstraat 86, 9000 Ghent (Belgium)
Fax: (+32) 9-264-66-97
E-mail: Veronique.Vanspeybroeck@UGent.be

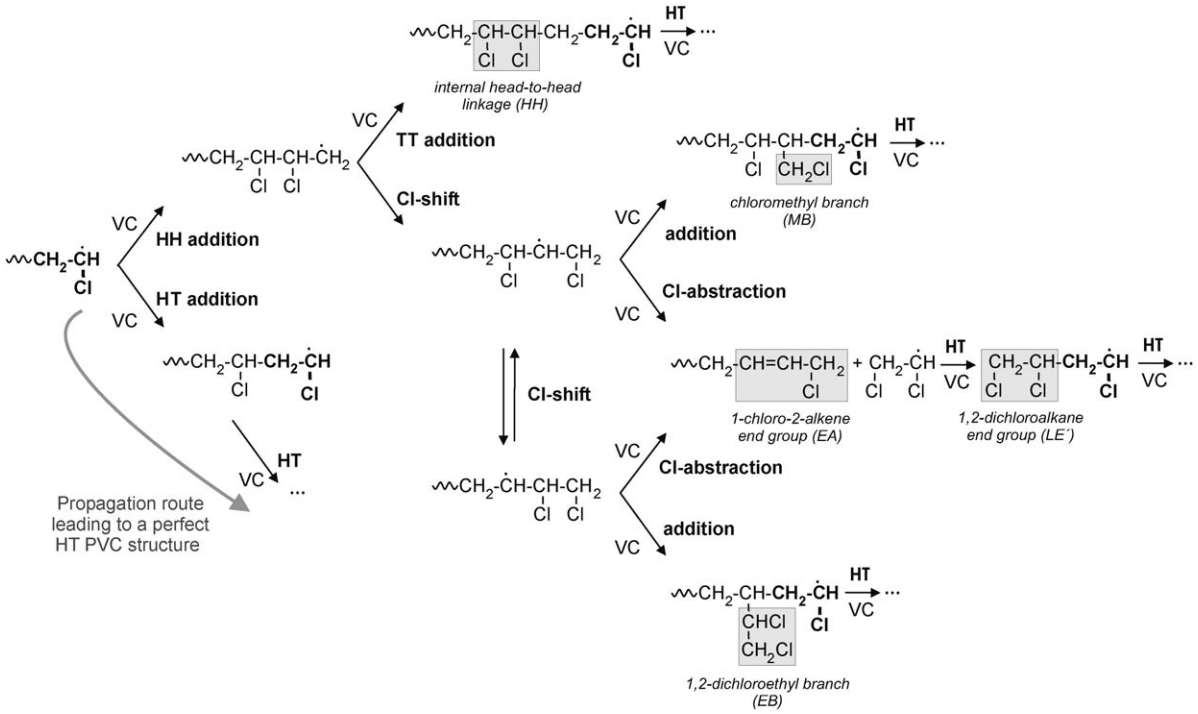

Scheme 1. Possible reaction pathways after a head-to-head addition, leading to a number of important defect structures in PVC.

cal. This reaction is referred to as the "1,2 Cl-shift", and is known to have a very low activation energy.[8] Further propagation from this radical center leads to the formation of a **chloromethyl branch** (MB, also called branch of type C_1). These $-CH_2Cl$ branches are the most frequent short chain branches in PVC (approximately 4/1000 VC units), as is shown by ^1H and ^{13}C NMR measurements.[8–11] It is accepted that this well-known type of defect structure is mainly introduced in the chain by the mechanism described above.[9,12] The methyl branch is not thermally unstable since there are no chlorine atoms bonded to the tertiary carbon.[3] Instead of further propagation after the Cl-shift, the chlorine attached to the third carbon atom can be abstracted by a monomer unit, producing an **1-chloro-2-alkene end group** (EA, end allylic structure).[9] The eliminated chlorine radical initiates a new polymer chain that differs from other chains by the typical **1,2-dichloroalkane end group**. This reaction is also referred to as chain transfer to monomer, and it is of great practical importance, as already mentioned. Other reaction mechanisms can be suggested for chain transfer to monomer, but the one discussed here was found to be the most important one.[9] A third possible reaction after the Cl-shift is a second Cl-shift of the chlorine atom on the third carbon atom to the second carbon atom. This radical can undergo reactions similar to those of the radical formed after the first Cl-shift, leading to the formation of an **ethyl branch** (EB, also called branch of type C_2) and the aforementioned end groups.[9] The saturated and unsaturated end groups shown in Scheme 1 are the most abundant end groups in PVC.[2,8]

The head-to-head addition followed by 1,2-chlorine migration was originally proposed by Rigo et al. for the formation of short chain branches in PVC, and later on confirmed by Starnes et al.[12,13] There is a consensus in the literature that the Cl-shift reaction proceeds rapidly, so most of the HH linkages formed in the chain by head-to-head additions will immediately disappear and lead to the formation of defect structures as described above.[8,12] Starnes even claims that the head-to-head radical does not add to monomer but always rearranges by a 1,2-chlorine shift of the β-chloro substituent.[7,9] The internal HH defect structures in PVC are believed to be formed mainly by another mechanism, that is, recombination of two propagating radical chains with a chlorine atom attached to the radical carbon (i.e. radicals formed by the head-to-tail mechanism; cf. Scheme 2).

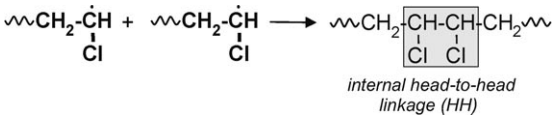

Scheme 2. Formation of internal head-to-head structures by recombination termination.

The extensive research on PVC polymerization reflects the enormous interest in this subject. Experimental data on the kinetics of this polymerization are readily available. Some averaged rate constants for the main polymerization steps (initiation, propagation, chain transfer to monomer and termination) have been derived by regression of experimental data for monomer conversion and molecular mass distribution as a function of reaction time and temperature.[14] Nevertheless, a comprehensive kinetic model which can accurately predict all prop-

erties of the synthesized polymer is still lacking due to the complexity of the polymerization process. In this respect, ab initio calculations on individual reaction steps can improve the fundamental insight into polymerization reactions, since all effects can be studied separately and the relative importance of competitive reaction paths can be estimated. Quantum mechanical molecular modeling techniques have often been applied in the field of polymer chemistry with the common goal of getting theoretical information on several aspects in a broad area of polymer systems [polyethylene (PE), poly(vinyl acetate) (PVA), polymethacrylonitrile (PMAN), polyacrylonitrile (PAN), acrylates, and so forth]. The studied aspects range from propagation kinetics, substituent effects, and solvent effects to properties of short chain branching. Relevant references published in this area during the last decade are the work of Radom,[15–17] Gilbert,[18–20] Heuts,[21,22] Aviyente,[23] and Coote[10] and their co-workers. Recently, a combined experimental and theoretical study was published concerning the formation of structural defects in PVC.[10] The monomer conversion dependence of the formation of various types of defects was measured by ^{1}H and ^{13}C NMR spectroscopy. Ab initio calculations were performed on four model reactions in an attempt to explain certain trends in the measured defect concentrations that could not be understood via the commonly accepted reaction schemes for the formation of structural defects in PVC. In a previous publication of our research group on free-radical polymerization, the chain length dependence of the propagation rate during the polymerization of polyethylene was investigated.[24]

The theoretical prediction of the kinetics is very sensitive to the level of theory which is used to model the electronic many-body problem. For PE, an in-depth level of theory study was performed to select cost-effective methods which are computationally feasible but yet also sufficiently accurate.[25] As PVC contains a heterogeneous element, the conclusions for the PE system may not a priori be extrapolated to PVC. Herein, a new level of theory study is performed for the addition of a methyl radical to vinyl chloride, for which experimental data are available.

In the second part, the selected level of theory is applied to study the kinetics of concurrent head-to-tail (HT) and head-to-head (HH) additions, with the aim of determining the relative importance of both reactions in terms of the chain length. A comparison is made with the available experimental data.

Finally, the head-to-head content is determined for other polymers with experimentally measured HH concentrations, that is, poly(vinyl fluoride) (PVF), poly(vinylidene fluoride) (PVDF) and PVA.

2. Computational Methods

2.1. Electronic Structure Calculations

All calculations were carried out with the Gaussian 03 software package.[26] As correlated wave function based methods such as CCSD(T) are not feasible for longer polymer chains, all levels of theory (LOT) applied in this work are based on density functional theory. The DFT-based methods in the LOT study can be categorized as follows:

- Two pure DFT methods are applied, namely BP86 and BLYP. For these methods gradient corrections have been introduced using the Becke exchange part (B) and either the Perdew (P86) or the Lee, Yang and Parr (LYP) correlation parts.[27–29]
- Hybrid Hartree–Fock density functional theory (so-called hybrid DFT) is set up by mixing various amounts of the Hartree–Fock (HF) nonlocal exchange operator with DFT exchange correlation functionals. Very promising hybrid functionals are B3LYP, B3PW91 and MPW1PW91,[30,31] since they have proven to be successful for obtaining accurate molecular geometries, vibrational frequencies and electronic energies.[32] The most important parameter that varies among these methods is the fraction of HF exchange, set to 20% in B3LYP and B3PW91 and 25% in MPW1PW91. The latter uses the modified Perdew–Wang exchange functional that has improved the long-range behavior as proposed by Adamo and Barone.[31] Other hybrid functionals used in this paper are BHandH and BHandHLYP which further vary by the amount of exact Hartree–Fock exchange that is taken into account and the explicit form for the correlation functional, which is in this case the LYP functional.[29,33] Also the more recent hybrid functional MPW1K proposed by Truhlar and co-workers was tested.[34] This modified Perdew–Wang one-parameter model for kinetics was optimized for a database of 20 forward barrier heights, 20 reverse barrier heights and 20 energies of reactions.
- In addition, a recently developed metafunctional by Boese and Martin for thermochemical kinetics was tested, that is, the BMK functional.[35]

The influence of the basis set on the results was tested by performing all DFT-based calculations with the double zeta 6-31G and triple zeta 6-311G basis in combination with extra polarization functions, leading to the 6-31G(d) and 6-311G(d,p) basis sets. Basis set saturation was further investigated by adding diffuse functions. All methods were combined with the 6-31+G(d) basis set and, for the best-performing methods, the 6-311++G(3df,2p) basis was also used. A recent article of Truhlar and co-workers highlights the effectiveness of diffuse basis functions for the calculation of relative energies by density functional theory.[36]

2.2. Reaction Kinetics

Within transition state theory (TST), the rate constant of a bimolecular reaction A+B→C is related to molecular properties of the reacting species [Eq. (1)]:[37,38]

$$k(T) = \frac{k_B T}{h} \frac{(q_{\pm}/V)}{(q_A/V)(q_B/V)} e^{-\frac{\Delta E_0}{k_B T}} \quad (1)$$

k_B represents the Boltzmann constant, T the absolute temperature, h the Planck constant and V the reference volume in

which the translational part of the partition function is evaluated. The molecular partition functions q_A and q_B relate to the two reactants and q_+ is the molecular partition function of the transition state. ΔE_0 represents the molecular energy difference at absolute zero between the activated complex and the reactants, with inclusion of the zero point vibrational energies.

The molecular properties, such as geometries, ground state energies and frequencies, that are required for the evaluation of the partition functions, and the reaction barrier ΔE_0 are obtained by the ab initio molecular calculations. All stationary points were localized by full geometry optimizations. The transition state structures were verified to have only one imaginary frequency.

The kinetic parameters are deduced from fitting the results of the TST expression [Eq. (1)] to the Arrhenius rate law [Eq. (2)] in a specific temperature range:

$$k(T) = Ae^{-E_a/RT} \quad (2)$$

Comparison of the TST expression with the Arrhenius rate law shows that the pre-exponential factor A is largely determined by the molecular partition functions, while the molecular energy difference ΔE_0 is a first-order approximation of the activation energy E_a.

3. Results and Discussion

3.1. Ab Initio Reaction Scheme

In this section, the ab initio kinetics are determined for the propagation reactions in Scheme 3. The polymerization is initiated by a methyl radical. This radical can add to the vinyl chloride monomer in two different ways: to the tail (CH_2 side) of VC (reaction PVC1_T), or to the head (CHCl side) of VC (reaction PVC1_H). The former produces a head-type radical (Cl is attached to the radical center) and the latter a tail-type radical (no Cl attached to the radical center). From this point on, we can distinguish four types of additions: head-to-tail and head-to-head (of a head-type radical) and tail-to-tail and tail-to-head (of a tail-type radical). These four reactions are schematically represented as HT, HH, TT and TH. The first H or T refers to the radical type while the second applies to the monomer side. The reaction PVC3_HT for instance refers to the third of three subsequent HT additions of VC to the methyl radical. To avoid a fast increase in the number of reactions per propagation step, we only consider reactions with the products of the HT and HH additions. As our calculations will show, the TT and TH reactions are of minor relevance. The level of theory study is performed on reaction PVC1_T. This is the addition of a methyl radical to vinyl chloride and models the initiation step of the free radical polymerization mechanism.

3.2. Level of Theory Study

Experimental gas-phase data for the studied initiation and propagation reactions shown in Scheme 3 are only available for PVC1_T, that is, the addition of a methyl radical to the tail-side of vinyl chloride.[39] This reaction is used to perform a level of theory study to validate which methods are cost-effective for the description of the first PVC propagation steps. The experimental data found in three references, Hogg and Kebarle (exp. 1), Kerr and Parsonage (exp. 2), and finally Tedder et al. (exp. 3) are reported in the first three columns of Table 1.[40] The rate constant given by Tedder et al. (exp. 3) is approximately a factor of 50 smaller than the rate constants found by Hogg and Kebarle (exp. 1) and Kerr and Parsonage (exp. 2). However Tedder et al. found a nice agreement of their measured relative rates with respect to the addition of a methyl radical to ethene with those of Hogg and Kebarle. It might be anticipated that the difference observed in absolute rates is due to the extrapolation to absolute rates. As the absolute rates of experiment 1 and experiment 2 agree well, we retained those two experiments for the level of theory validation. The experiments were conducted in the limited temperature range 390–440 K, and the comparison with the theoretical rate constant is consequently made in this restricted interval. The rejection of experiment 3 will be justified by the ab initio data.

The validation of the accuracy of a theoretical method for the prediction of the kinetics of the studied reaction is based upon the reproduction of the rate constant rather than on the reproduction of the activation energy and the pre-exponential factor, due to the inaccuracies in extracting numerical estimates for these quantities. To illustrate this, the difference in the experimental activation energies of Hogg and Kebarle (exp. 1) and Kerr and Parsonage (exp. 2) amounts to 14 kJ mol^{-1}, while the global rate constant only deviates over a factor of 1.4 on average. This large discrepancy is partly attributed to the narrow temperature range in which the experiments were carried out, invoking a large extrapolation to deduce the Arrhenius kinetic parameters.

To quantify the deviation of the theoretical rate constant with respect to the experimental value, an assessment is made on basis of the ratio $f_k = k_{theory}/k_{experiment}$. In ab initio applications a theoretical method is deemed to be acceptable if the deviation from the experiment is less than a factor 10, that is, $0.1 < f_k < 10$.[25]

Results

The quantitative values of the rate constant and the activation energy in the temperature range 390–440 K are presented in Table 1. Also, the ratio $f_k = k_{theory}/k_{experiment}$ is given for both experiments, averaged over the temperature interval. We notice that B3LYP, B3PW91, and MPW1K perform very well; MPW1PW91, BMK and BLYP perform well for some basis sets and BHandH, BP86, and BHandHLYP perform poorly.

The basis set dependence is quite uniform for all methods: the rate constant decreases when extending the basis set from 6-31G(d) to 6-311G(d,p) and the inclusion of diffuse functions lowers the rate constant even more. This confirms the conclusion of Truhlar et al. about the effectiveness of diffuse basis functions.[36] A further decrease is seen when using the extended basis set 6-311++G(3df,2p). The latter basis set was only applied for the well-performing functionals (B3LYP, B3PW91,

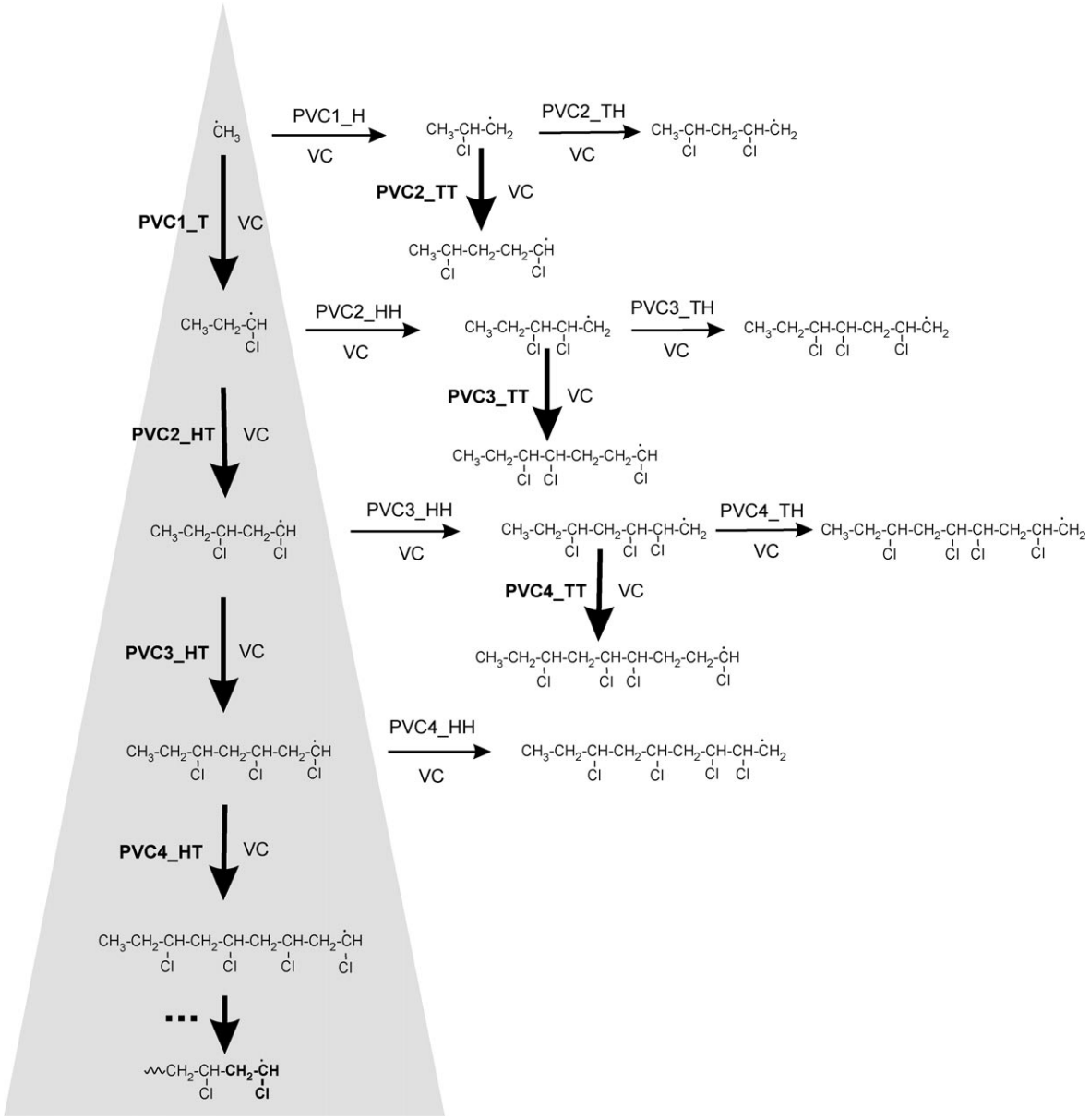

Scheme 3. Schematic representation of the studied head-to-tail and head-to-head propagation reactions of PVC. The vertical arrows (bold) are the preferential reaction routes. The pyramid represents the head-to-tail (HT) propagation route leading to a perfectly regular HT polymer.

MPW1PW91, MPW1K, BMK). The success of diffuse functions for PVC is related to the electronegativity of the element chlorine, which is better described with additional diffuse functions.

As already mentioned, a deviation of a factor 10 is the maximum tolerance for the LOT in reproducing the rate constant. All levels of theory satisfying this condition are potentially acceptable and are shown as green boxes in the overview given in Figure 1. An assessment with respect to experiment 1[40a] or experiment 2[40b] leads to the following conclusions: the best-performing methods are B3LYP/6-31+G(d), B3LYP/6-311G(d,p), B3PW91/6-31+G(d,p), B3PW91/6-311++G(3df,2p) and MPW1K/6-31+G(d).

The computational cost required by each of the selected methods can vary substantially, hence it can be used as an additional parameter in the final selection of the most suitable LOT for the study of PVC propagation reactions. Increasing basis set size leads to an increase of the computational cost. Adding diffuse functions (6-31+G(d), BS2) doubles the computational cost, while it is even a factor of 20 greater for the largest triple-zeta basis set including diffuse functions (6-311++G-(3df, 2p), BS4). Taking into account the above computational cost considerations, only the B3LYP/6-31+G(d), B3PW91/6-31+G(d,p) and MPW1K/6-31+G(d) are retained as cost-effective methods for the study of the propagation kinetics during PVC polymerization. The B3LYP/6-31+G(d) method is used throughout this paper.

Table 1. Rate constant of the addition of a methyl radical to vinyl chloride (PVC1_T, Scheme 3) for the level of theory (LOT) study (k in $m^3 mol^{-1} s^{-1}$).[a]

	exp. 1[40a]	exp. 2[40b]	exp. 3[40c]	B3LYP				B3PW91				BHandH			BHandHLYP		
				BS1	BS2	BS3	BS4	BS1	BS2	BS3	BS4	BS1	BS2	BS3	BS1	BS2	BS3
T [K]	Rate constant ln(k), k [$m^3 mol^{-1} s^{-1}$]																
390	3.62	4.21	−0.21	5.28	3.68	4.07	3.29	5.35	4.13	4.42	3.89	11.39	10.01	10.35	2.98	1.54	1.57
400	3.92	4.41	0.10	5.47	3.92	4.29	3.53	5.55	4.36	4.64	4.13	11.44	10.09	10.43	3.22	1.82	1.85
410	4.21	4.60	0.41	5.66	4.14	4.51	3.77	5.74	4.58	4.85	4.35	11.50	10.17	10.50	3.46	2.08	2.12
420	4.49	4.78	0.69	5.84	4.36	4.71	3.99	5.92	4.79	5.05	4.57	11.55	10.25	10.57	3.68	2.34	2.37
430	4.76	4.95	0.97	6.01	4.56	4.91	4.21	6.09	4.99	5.24	4.77	11.60	10.33	10.64	3.89	2.58	2.61
440	5.01	5.11	1.23	6.18	4.76	5.10	4.42	6.26	5.18	5.43	4.97	11.65	10.40	10.71	4.10	2.82	2.85
				E_a [$kJ mol^{-1}$]													
	39.7	25.9	41.0	25.7	30.7	29.5	32.2	26.0	29.9	28.8	30.8	7.6	11.1	10.3	31.8	36.5	36.4
			Error analysis														
			$< f_k^{exp\,1} >$	4.13	0.91	1.31	0.63	4.46	1.41	1.84	1.12	1427	377	524	0.46	0.12	0.12
			$< f_k^{exp\,2} >$	2.90	0.65	0.93	0.45	3.13	1.00	1.30	0.80	966	257	356	0.33	0.08	0.09
			$< f_k^{<exp>} >$	3.51	0.78	1.12	0.54	3.80	1.21	1.57	0.96	1197	317	440	0.39	0.10	0.10

	exp. 1[40a]	exp. 2[40b]	exp. 3[40c]	BLYP			BP86			MPW1PW91				MPW1K		BMK	
				BS1	BS2	BS3	BS1	BS2	BS3	BS1	BS2	BS3	BS4	BS2	BS4	BS2	BS4
T [K]	Rate constant ln(k), k [$m^3 mol^{-1} s^{-1}$]																
390	3.62	4.21	−0.21	7.30	5.44	6.08	9.00	7.58	8.48	7.54	4.92	5.24	4.51	3.77	3.33	3.11	2.48
400	3.92	4.41	0.10	7.46	5.64	6.26	9.12	7.73	8.62	7.69	5.13	5.44	4.73	4.00	3.57	3.35	2.74
410	4.21	4.60	0.41	7.61	5.83	6.44	9.24	7.89	8.75	7.82	5.32	5.63	4.94	4.22	3.81	3.59	2.99
420	4.49	4.78	0.69	7.75	6.02	6.61	9.36	8.03	8.89	7.95	5.51	5.81	5.14	4.43	4.03	3.81	3.23
430	4.76	4.95	0.97	7.89	6.20	6.77	9.48	8.17	9.01	8.08	5.70	5.98	5.33	4.63	4.24	4.03	3.45
440	5.01	5.11	1.23	8.03	6.37	6.93	9.59	8.31	9.14	8.19	5.87	6.15	5.52	4.83	4.45	4.24	3.67
				E_a [$kJ mol^{-1}$]													
	39.7	25.9	41.0	20.6	26.4	24.2	16.8	20.8	18.8	18.7	27.1	26.0	28.6	30.0	31.7	32.2	33.9
			Error analysis														
			$< f_k^{exp\,1} >$	29	4.93	9.00	149	38	91	36	2.96	4.00	2.02	0.99	0.65	0.53	0.29
			$< f_k^{exp\,2} >$	20	3.46	6.29	102	27	63	25	2.08	2.81	1.43	0.70	0.46	0.37	0.21
			$< f_k^{<exp>} >$	25	4.19	7.65	125	32	77	30	2.52	3.40	1.72	0.84	0.56	0.45	0.25

[a] E_a is the activation energy ($kJ mol^{-1}$). The experimental data are from Hogg and Keblare (exp. 1), Kerr and Parsonage (exp. 2) and Tedder et al. (exp. 3).[40] The latter is not taken into account for the error analysis due to the large deviation from experiment 1 and experiment 2. f_k is the ratio of the theoretical over the experimental rate constant ($< exp >$ is the averaged value of exp. 1 and exp. 2). The basis sets are 6-31G(d) (BS1), 6-31+G(d) (BS2), 6-311G(d,p) (BS3) and 6-311++G(3df,2p) (BS4).

Influence of Internal Rotations

The rotation about the forming bond in the transition state of the benchmark reaction PVC1_T corresponds to a low vibrational frequency [84 cm^{-1} for B3LYP/6-31+G(d)]. We applied the one-dimensional hindered rotor (1D-HR) method to this rotation. More theoretical details can be found in the work of Van Speybroeck et al.[41] The correction factor q^{IR}/q^{HO} for the rotational partition function with respect to the harmonic oscillator description amounts to 1 based on the B3LYP/6-31+G(d) rotational potential. This means that the harmonic oscillator predictions in the above LOT are not altered and the conclusions about the cost-effective methods remain valid. A similar effect was found in the LOT study on elementary reactions of PE, for the addition of a methyl radical to ethene.[25]

3.3. Head-to-Tail versus Head-to-Head Additions

Ab Initio Kinetics

In this section, the kinetic results for the Scheme 3 (introduced in section 3.1) are discussed. For all studied reactions the rate constant and derived kinetic parameters in the temperature interval 270–390 K are presented in Table 2. The transition state structures of two competitive reaction couples for the fourth addition step (PVC4_HT, PVC4_HH) and (PVC4_TH, PVC4_TT)

	exp.1	exp.2	<exp>
B3LYP/6-31G(d)	4.1	2.9	3.5
B3LYP/6-31+G(d)	**0.91**	**0.65**	**0.78**
B3LYP/6-311G(d,p)	**1.3**	**0.93**	**1.1**
B3LYP/6-311++G(3df,2p)	0.63	0.45	0.54
B3PW91/6-31G(d)	4.5	3.1	3.8
B3PW91/6-31+G(d)	**1.4**	**1.0**	**1.2**
B3PW91/6-311G(d,p)	1.8	1.3	1.6
B3PW91/6-311++G(3df,2p)	**1.1**	**0.80**	**0.96**
BHandH/6-31G(d)			
BHandH/6-31+G(d)			
BHandH/6-311G(d,p)			
BHandHLYP/6-31G(d)	0.46	0.33	0.39
BHandHLYP/6-31+G(d)	0.12		0.10
BHandHLYP/6-311G(d,p)	0.12		0.10
BLYP/6-31G(d)			
BLYP/6-31G+(d)	4.9	3.5	4.2
BLYP/6-311G(d,p)	9.0	6.3	7.7
BP86/6-31G(d)			
BP86/6-31G+(d)			
BP86/6-311G(d,p)			
MPW1PW91/6-31G(d)			
MPW1PW91/6-31+G(d)	3.0	2.1	2.5
MPW1PW91/6-311G(d,p)	4.0	2.8	3.4
MPW1PW91/6-311++G(3df,2p)	2.0	1.4	1.7
MPW1K/6-31+G(d)	**0.99**	**0.70**	**0.84**
MPW1K/6-311++G(3df,2p)	0.65	0.46	0.56
BMK/6-31+G(d)	0.53	0.37	0.45
BMK/6-311++G(3df,2p)	0.29	0.21	0.25

Figure 1. Schematic overview of the error analysis on reaction PVC1_T (< exp >: averaged value of exp. 1 and exp. 2). The numbers indicated in the green boxes represent $<f_k>$ in the temperature range 390–440 K. The best-performing methods are in bold, the cost-effective methods are accentuated bold boxes.

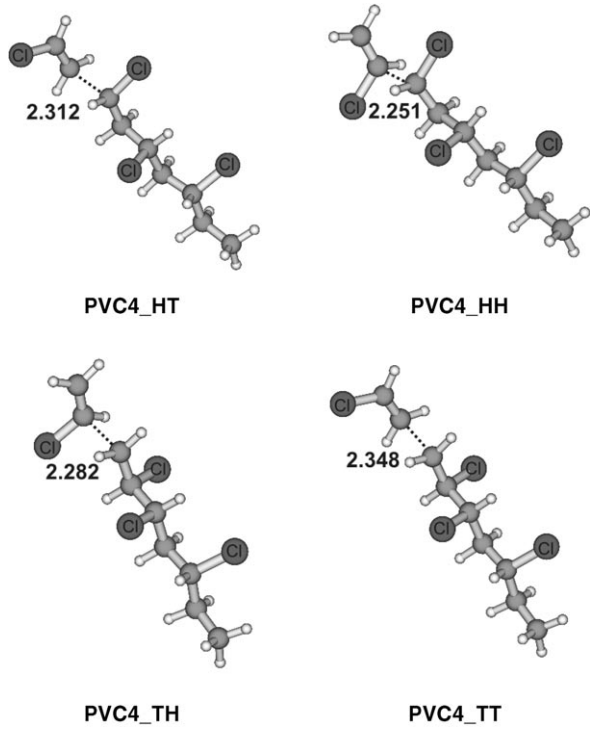

Figure 2. Transition state structures of concurring reactions PVC4_HT and PVC4_HH, and concurring reactions PVC4_TH and PVC4_TT. The length of the forming bond is given in Ångström.

are depicted in Figure 2. A typical HH addition has an activation energy that is substantially higher than the corresponding HT addition ($\Delta E_a \simeq 15\ kJ\,mol^{-1}$ for the fourth addition). The preference for the head-to-tail addition can be understood since in the product of a typical HT addition, the free radical is located on the head end and the substituent is able to provide stabilization to the carbon atom bearing the unpaired electron. Secondary or tertiary radicals are known to be more stable than primary radicals due to the inductive influence of the substituent. A further factor that favors the HT addition over the HH addition is that steric hindrance is less pronounced when a propagating radical approaches the unsubstituted carbon atom of the monomer.[43]

Taking a closer look at Scheme 3 shows that each reaction product of a VC addition can react in two competitive ways. The abundance of a certain reaction product can be directly related to the reaction rate constant. Considering two competitive reaction routes "1" and "2", the probabilities of both pathways relate to the reaction rates as follows [Eq. (3)]:

$$p_1 = \frac{r_1}{r_1 + r_2},\ p_2 = \frac{r_2}{r_1 + r_2} \qquad (3)$$

The reaction rate r_i is a function of the concentrations of the reacting species (i.e. the propagating radical R_n and the VC monomer) and of the reaction rate coefficient: $r_i = k_i c_{VC} c_{R_n}$. The rate coefficient can be determined by ab initio procedures as described in section 2. Since both competitive reaction routes "1" and "2" start from the same reacting species, the expressions of the reaction pathway probabilities reduce to [Eq. (4)]:

$$p_1 = \frac{r_1}{r_1 + r_2} = \frac{k_1 c_{VC} c_{R_n}}{k_1 c_{VC} c_{R_n} + k_2 c_{VC} c_{R_n}} = \frac{k_1}{k_1 + k_2},\ p_2 = \frac{k_2}{k_1 + k_2} \qquad (4)$$

with k_i the intrinsic reaction rate coefficient as determined theoretically.

The probabilities of the competitive reaction paths in Scheme 3—determined by application of Equation (3) to the ab initio kinetic data—are presented in Table 2. For the first VC addition (to the methyl radical), the competitive reaction routes are PVC1_T and PVC1_H. The kinetic data show that the PVC1_T reaction has a much lower activation energy ($\Delta E_a \simeq 15\ kJ\,mol^{-1}$) and a pre-exponential factor which is approximately three times larger. This leads to a probability of 99.85% for reaction PVC1_T and 0.15% for reaction PVC1_H. Reaction PVC1_T can be followed by the competitive reactions PVC2_HT or PVC2_HH, whereas reaction PVC1_H can be followed by the competitive reactions PVC2_TT or PVC2_TH. The kinetic data of the latter reactions are of minor importance compared to PVC2_HT and PVC2_HH, since they follow the rare event of a PVC1_T addition. It is, however, instructive to learn that a head-to-head addition is preferentially followed by a tail-to-tail addition (99.7% probability), restoring the head-type propagating radical (cf. Scheme 1). In Scheme 3 the preferred reactions

Table 2. Kinetic parameters and derived probabilities of the studied head-to-head and head-to-tail reactions (cf. Scheme 3).[a]

	PVC1_T	PVC1_H	PVC2_HT	PVC2_HH	PVC3_HT	PVC3_HH	PVC4_HT	PVC4_HH
ΔE_0	27.35	42.83	29.61	44.60	30.03	45.43	30.20	45.22
E_a	29.10	43.96	33.56	48.27	34.42	49.72	34.60	49.50
A	3.13E+5	1.04E+5	7.71E+03	2.17E+3	6.21E+3	3.21E+3	4.87E+3	2.41E+3
$k^{330\,K}$	7.63E+0	1.13E−2	3.69E−2	4.87E−5	2.17E−2	4.25E−5	1.60E−2	3.46E−5
$p^{330\,K}$	0.9985	0.0015	0.9987	**0.0013**	0.9980	**0.0020**	0.9978	**0.0022**
variation of the reaction probability with temperature:								
T [K]								
270	0.9996	0.0004	0.9996	**0.0004**	0.9994	**0.0006**	0.9993	**0.0007**
300	0.9991	0.0009	0.9992	**0.0008**	0.9989	**0.0011**	0.9987	**0.0013**
330	0.9985	0.0015	0.9987	**0.0013**	0.9980	**0.0020**	0.9978	**0.0022**
360	0.9977	0.0023	0.9979	**0.0021**	0.9969	**0.0031**	0.9966	**0.0034**
390	0.9966	0.0034	0.9970	**0.0030**	0.9954	**0.0046**	0.9950	**0.0050**
	PVC7_HT	PVC7_HH	PVC2_TH	PVC2_TT	PVC3_TH	PVC3_TT	PVC4_TH	PVC4_TT
ΔE_0	30.28	45.33	48.55	36.88	50.51	37.49	49.84	36.37
E_a	34.84	49.68	52.15	40.93	54.34	41.84	53.75	40.72
A	6.04E+3	2.85E+3	3.35E+3	1.99E+4	2.62E+3	2.09E+4	2.46E+3	1.68E+4
$k^{330\,K}$	1.81E−2	3.82E−5	1.83E−5	6.51E−3	6.45E−6	4.89E−3	7.51E−6	5.93E−3
$p^{330\,K}$	0.9979	**0.0021**	2.81E−03	9.97E−01	1.32E−03	9.99E−01	1.27E−03	9.99E−01
variation of the reaction probability with temperature:								
T [K]								
270	0.9994	**0.0006**	0.0011	0.9989	0.0005	0.9995	0.0004	0.9996
300	0.9988	**0.0012**	0.0019	0.9981	0.0008	0.9992	0.0008	0.9992
330	0.9979	**0.0021**	0.0028	0.9972	0.0013	0.9987	0.0013	0.9987
360	0.9967	**0.0033**	0.0039	0.9961	0.0019	0.9981	0.0019	0.9981
390	0.9952	**0.0048**	0.0053	0.9947	0.0026	0.9974	0.0026	0.9974

[a] ΔE_0 represents the reaction barrier at 0 K with inclusion of the zero-point energy (ZPE) and is expressed in kJ mol^{-1}. E_a is the activation energy (kJ mol^{-1}) and A the pre-exponential factor (m^3 mol^{-1} s^{-1}) as figuring in the Arrhenius rate law. k is the reaction rate constant (m^3 mol^{-1} s^{-1}) and p is the probability of the reaction with respect to its concurrent reaction. The bold numbers are the probabilities of head-to-head addition with respect to head-to-tail propagation.

are displayed vertically, while the less favorable reactions are arranged horizontally. It should be stressed that a head-to-head addition is in most cases followed by a Cl-shift (Scheme 1) as discussed in the introduction, so only the relative importance of the HT and HH reactions is of practical relevance. Table 2 indicates that the probability of a head-to-head addition (bold numbers) of the polymeric radical to VC is about 0.2% from the third monomer addition on, which means that—at least according to ab initio predictions—2 out of 1000 VC additions will be head-to-head additions. Additional calculations on reactions PVC7_HT and PVC7_HH with a chain length of 15 carbon atoms in the transition state confirms the convergence of this number in terms of the chain length (cf. Table 2).

Another aspect that emerges from Table 2 is the variation of the HH probability with temperature. The probability of head-to-head addition increases rapidly in terms of the polymerization temperature. A deviation of 30 °C from the average polymerization temperature of 330 K changes the probability of HH addition by a factor of 1.5. This is due to the substantial difference in activation energy of HT and HH additions mentioned before.

Experimental Data

As discussed in the introduction, most of the HH structures formed in the chain by head-to-head additions will immediately disappear through Cl-shift reactions leading to the formation of defect structures as illustrated in Scheme 1. The internal HH linkages in PVC are mainly formed by another mechanism, that is, recombination termination of two propagating radical chains with a chlorine atom attached to the radical carbon, as shown in Scheme 2. These two effects imply that we cannot relate the frequency of head-to-head addition determined via ab initio techniques (2 per 1000 VC additions at 330 K) to the number of internal HH linkages, as experimentally measured. To validate our theoretical probability of head-to-head propagation, an indirect comparison with the experimental quantities of defect structures formed after head-to-head addition is made (Scheme 1). The frequencies of occurrence of all structural defects in PVC are quite low, the most abundant effect is the methyl branch (~4 per 1000 VC units). The literature data for the defect structures formed after head-to-head addition of VC to the polymeric radical are summarized in Table 3. The concentration of defect structures can be estimated directly by use of NMR spectroscopy, however, for the HH linkages it is be-

Table 3. Experimental concentrations of defect structures formed after head-to-head addition (cf. Scheme 3), in numbers per 1000 monomer units.

	Type of defect	Experimental data	References
HH	internal HH linkage	<0.2	<0.2[8]
MB	chloromethyl branch (tertiary H)	3.3–5.8	3.8–4.4[4], 3.3–4.8[5], 4.5[10], 5.8[44], 3.8[46]
EA	1-chloro-2-alkene end group	0.45–0.95[a]	0.7[a][4], 0.45[a][10], 0.75[a][46], 0.85–0.95[a][47]
LE′	1,2-dichloroalkane end group	0.8–0.9[a]	0.8–0.9[a][4]
EB	1,2-dichloroethyl branch	0.14–0.55	0.14–0.55[5], 0.4[10], 0.4[44]

[a] The end group structures EA and LE′ are expressed in number per molecule. The results are obtained by NMR techniques (^{1}H and ^{13}C) at 55 °C,[4,8,46] at 57.5 °C,[10] at 82 °C,[44] at 30–80 °C,[47] or at unknown *T*.[5]

neath the detection limit of 2 per 1000 monomeric units.[8] The number of HH linkages has been determined by a chemical method, leading to concentrations of 2.5–7 per 1000 monomeric units, increasing with the polymerization temperature.[42] According to Hjerberg et al., the discrepancy between these results is due to the incorporation of the number of saturated 1,2-dichloro-end groups (LE′) that are formed after chain transfer to monomer (cf. Scheme 1). They estimated the true concentration of internal HH linkages to be less than 0.2 per 1000 monomeric units.[8] The experimental error in the ^{13}C NMR spectroscopy is about 0.1 defects/1000 VC units.[10]

A rough comparison between the concentrations of defects in Scheme 1 and the probability of head-to-head propagation can be made as follows. A first approximation consists of neglecting the probability of further TT propagation after a HH addition, as has been suggested in the literature.[7] This means that the Cl-shift will always take place. A second approximation is made by assuming that the structural defects in Scheme 1 (methyl branch, ethyl branch, chloroallylic end group and 1,2-dichloroalkane end group) only appear in the PVC structure as a result of HH additions. Although alternative reaction routes leading to the formation of chloromethyl branches have been suggested in literature, the HH route is generally accepted as the dominant mechanism at normal conversions.[10] Also, chain transfer to monomer, leading to the 1,2-dichloroalkane end group, can proceed by alternative reaction mechanisms, but those are of minor importance.[9] Table 3 shows that the concentration of chloroallylic end groups and 1,2-dichloroalkane end groups is approximately equal, supporting the previously mentioned approximations. These approximations lead to the following relation: $p(\text{HH addition}) \sim c(\text{MB}) + c(\text{EB}) + c(\text{EA})$. This means that the estimated probability of HH addition based on the experimental defect concentrations (Table 3) is between 4.0 and 7.6 per 1000 VC additions. This value is only a rough approximation of the number of HH additions per 1000 VC units. The concentrations of structural defects measured by NMR spectroscopy depend on monomer conversion, temperature, polymerization technique (bulk, suspension, etc.) and are somewhat scattered around the reference values (Table 3). The approximations made above can lead to discrepancies between the actual rate of HH addition and the estimated one.

The theoretical prediction of 2 HH additions per 1000 VC units is in the correct order of magnitude and lies within the possible errors of the experimental estimate, due to the reasons described above.

Comparing the temperature dependence of the HH probability in Table 2 with the experimentally measured variation shows a very good agreement: in ref. [44] a reaction temperature of 82 °C led to 5.8 MB/1000 VC, while the value in ref. [10] at 57.15 °C was 3.8 (factor of 1.5 increase, as predicted by theory!).

Importance of HH Linkages in Other Polymers

For poly(vinyl chloride), the occurrence of HH additions is of practical relevance, despite its low probability, since it leads to the formation of defect structures in the polymer. Head-to-head linkages have been directly measured for a number of other polymeric systems where the occurrence is more abundant. Although not historically first observed, the most notable cases of the direct incorporation of HH linkages are polymers from fluorine substituted α-olefins. [43] These fluorocarbon polymers have attracted attention, since they can be studied not only by ^{13}C and ^{1}H NMR spectroscopy but also by ^{19}F NMR spectroscopy. Wilson and Santee found approximately 10% HH linkages for PDVF and 30% HH linkages for PVF.[45] It is now generally accepted that the small size of the fluorine atom can account for this ease of the reverse addition. The small amount of steric influence and the relatively poor resonance stabilization ability of the fluorine atom probably combine to allow for the formation of HH linkages.[43] The concentration of HH linkages was also determined for PVA: 1.5% at 60 °C and 2.0% at 100 °C.[48]

Ab initio predictions of the number of HH additions were derived for PVF, PVDF and PVA from reactions equivalent to PVC2_HT and PVC2_HH (cf. Scheme 3). The transition state structures are given in Figure 3 and the kinetics are summarized in Table 4. Note that in the case of PVDF, the *trans* conformation for the head-to-tail attack is not stable due to the electrostatic repulsion of the two fluorine atom pairs at the same side of the carbon backbone. A *cis*-like conformation is energetically stable since it maximizes the distances between the fluorine atoms. Table 4 shows that the energetic differences for HH compared to HT addition are 15, 3.4, 6.3 and 17 kJ mol^{-1} for PVC, PVF, PVDF and PVA, respectively. The low values for PVF and PVDF are reflected in high HH contents as experimentally observed. PVDF has a lower HH content due to the extra stability of the *cis*-like transition state for HT addition. The similar energy values for PVC and PVA cannot be extrapolated to similar HH contents since the frequency factor has a different behavior. According to our ab initio method, 0.13, 9.1, 2.3 and 1.7% of the monomer units are added in a head-to-head fashion at 330 K for PVC, PVF, PVDF and PVA, respectively. This can be compared to the experimentally measured HH contents of 0.5, 30, 10 and 1.5% (indirect estimate for PVC based on the

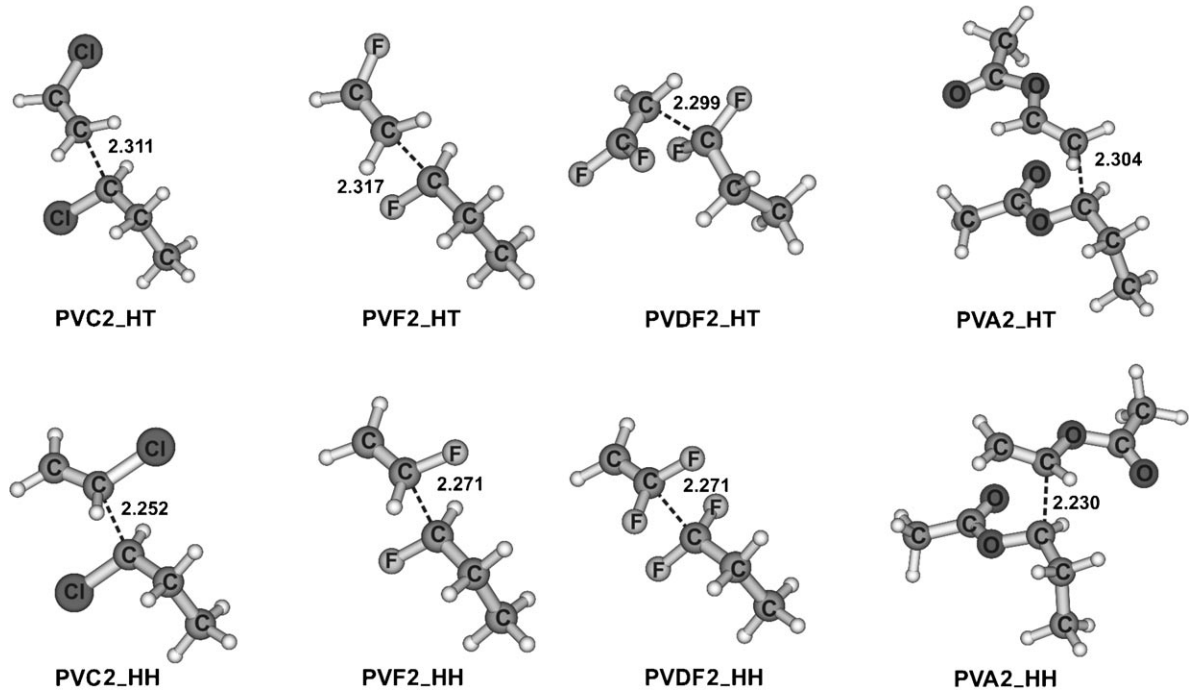

Figure 3. Transition state structures of the second head-to-head and head-to-tail additions for poly(vinyl chloride) (PVC), poly(vinyl fluoride) (PVF), poly(vinylidene fluoride) (PVDF) and poly(vinyl acetate) (PVA). The length of the forming bond is given in Ångström.

Table 4. Kinetic parameters and derived probabilities of the head-to-head and head-to-tail reactions for PVC, PVF, PVDF and PVA.[a]

	PVC2_HT	PVC2_HH	PVF2_HT	PVF2_HH	PVDF2_HT	PVDF2_HH	PVA2_HT	PVA2_HH
ΔE_0	29.61	44.60	27.44	31.12	22.11	28.41	26.70	42.76
E_a	33.56	48.27	31.84	35.27	27.97	34.27	30.12	46.81
A	7.71E+3	2.17E+3	2.28E+4	8.01E+3	2.73E+4	6.37E+3	1.78E+2	1.36E+3
$k^{330\,K}$	3.69E−2	4.87E−5	2.04E−1	2.05E−2	9.98E−1	2.34E−2	2.98E−3	5.20E−5
$p^{330\,K}$	0.9987	**0.0013**	**0.9089**	**0.0911**	**0.9771**	**0.0229**	0.9829	**0.0171**
variation of the reaction probability with temperature:								
T [K]								
270	0.9996	**0.0004**	0.9293	**0.0707**	0.9860	**0.0140**	0.9955	**0.0045**
300	0.9992	**0.0008**	0.9187	**0.0813**	0.9817	**0.0183**	0.9906	**0.0094**
330	0.9987	**0.0013**	0.9089	**0.0911**	0.9771	**0.0229**	0.9829	**0.0171**
360	0.9979	**0.0021**	0.8999	**0.1001**	0.9724	**0.0276**	0.9719	**0.0281**
390	0.9970	**0.0030**	0.8915	**0.1085**	0.9676	**0.0324**	0.9574	**0.0426**

[a] ΔE_0 represents the reaction barrier at 0 K with inclusion of the zero-point energy (ZPE) and is expressed in kJ mol^{-1}. E_a is the activation energy (kJ mol^{-1}) and A the pre-exponential factor (m^3 mol^{-1} s^{-1}) in the Arrhenius rate law. k is the reaction rate constant (m^3 mol^{-1} s^{-}) and p is the probability of the reaction with respect to its concurrent reaction.

defect concentrations in Table 3). Ab initio methods underestimate the true HH concentration—exept for PVA where the value is reproduced almost exactly—but the relative order of head-to-head probability between the different polymers is correctly predicted. We recall that in the case of PVF, PVDF, and PVA the experimental HH concentration can also contain a contribution from termination recombination. However, this contribution is very minor since a polymer chain can only contain one extra HH linkage due to recombination termination. Given an average chain length of 1000 monomer units, recombination could only contribute about 0.1 % to the total HH content, which is negligible considering the experimental concentrations. The underestimation of the experimental HH concentration must thus be related to the relative underestimation of HH propagation compared with HT propagation on ab initio basis. An increase in the chain length of the ab initio model could be (partially) responsible for this underestimation. Indeed, in the case of PVC, an increase by a factor of 1.7 is noticed when going from a chain length of 2 (PVC2_HT and PVC2_HH) to the higher chain lengths (cf. Table 2). Another possible reason for the underestimation is that the ab initio calculations are carried out in the gas phase, while the polymerization of the above discussed monomers takes place in the liquid phase. However, unless solvent effects are substantially different for the HH and HT reaction, this approximation is not likely to affect the predicted HH content.

4. Conclusions

The relative importance of head-to-head versus head-to-tail additions during the propagation of poly(vinyl chloride) is deter-

mined by ab initio methods for different chain lengths of the polymer. Prior to this work, a systematic level of theory study on the addition of a methyl radical to the tail side of vinyl chloride is performed. This reaction is one of the elementary reaction steps during the propagation of PVC, and the only one for which experimental gas-phase data are available. Based on this LOT study, a number of cost-effective methods are selected that give a good reproduction of the reaction rate in a computationally efficient way. The studied methods are all DFT based. Comparison with the experimental rate constant points out that B3LYP, B3PW91 and MPW1K combined with the 6-31+G(d) basis set are suitable cost-effective methods for studying PVC propagation reactions.

In a second part of the paper, the B3LYP/6-31+G(d) level of theory is used to study the relative importance of head-to-head and head-to-tail additions for the first propagation steps of PVC polymerization. Although the PVC propagation proceeds mainly via the head-to-tail mechanism, the rare event of a head-to-head addition is very important since it gives rise to the formation of defect structures. Our theoretical prediction of the probability of head-to-head addition is 2 per 1000 VC additions. An indirect comparison with the experimental concentrations of defect structures formed after an HH addition shows that this is in the correct order of magnitude.

Finally, similar calculations were performed for poly(vinyl fluoride) (PVF), poly(vinylidene fluoride) (PVDF) and poly(vinyl acetate) (PVA). For the fluorine-substituted monomers, large amounts of HH content have been measured experimentally. The PVA case was taken up as a reference monomer with a larger substituent. The relative abundance of HH units in both fluorine-substituted polymers is correctly reproduced by our theoretical calculations. The HH content of PVA is predicted within the experimental uncertainties.

Acknowledgements

This work was supported by the Fund for Scientific Research—Flanders (FWO) and the Fund for Scientific Research of the Ghent University.

Keywords: density functional calculations · head-to-head additions · polymerization · radical reactions · vinyl chloride

[1] D. Braun, *J. Polym. Sci. Part A* **2004**, *42*, 578.
[2] T. Y. Xie, A. E. Hamielec, P. E. Wood, D. R. Woods, *Polymer* **1991**, *32*, 537.
[3] K. Endo, *Prog. Polym. Sci.* **2002**, *27*, 2021.
[4] T. Hjertberg, E. M. Sorvik, *Polymer* **1983**, *24*, 673.
[5] M. Rogestedt, T. Hjertberg, *Macromolecules* **1993**, *26*, 60.
[6] T. Y. Xie, A. E. Hamielec, M. Rogestedt, T. Hjertberg, *Polymer* **1994**, *35*, 1526.
[7] W. H. Starnes, Jr., *Prog. Polym. Sci.* **2002**, *27*, 2133.
[8] T. Hjertberg, E. Sorvik, A. Wendel, *Makromol. Chem. Rapid Commun.* **1983**, *4*, 175.
[9] W. H. Starnes, Jr., *J. Polym. Sci. Part A* **2005**, *43*, 2451.
[10] J. Purmova, K. F. D. Pauwels, W. van Zoelen, E. J. Vorenkamp, A. J. Schouten, M. L. Coote, *Macromolecules* **2005**, *38*, 6352.
[11] a) A. Guyot, *Macromolecules* **1986**, *19*, 1090; b) M.-F. Llauro-Darricades, N. Bensemra, A. Guyot, R. Pétiaud, *Macromol. Chem. Macromol. Symp.* **1989**, *29*, 171.
[12] W. H. Starnes, Jr., F. C. Schilling, K. B. Abbås, R. E. Cais, F. A. Bovey, *Macromolecules* **1979**, *12*, 556.
[13] A. Rigo, G. Palma, G. Talamini, *Makromol. Chem.* **1972**, *153*, 219.
[14] T. De Roo, J. Wieme, G. J. Heynderickx, G. B. Marin, *Polymer* **2005**, *46*, 8340.
[15] J. P. A. Heuts, R. G. Gilbert, L. Radom, *Macromolecules* **1995**, *28*, 8771.
[16] J. P. A. Heuts, R. G. Gilbert, L. Radom, *J. Phys. Chem.* **1996**, *100*, 18997.
[17] M. L. Coote, L. Radom, *Macromolecules* **2004**, *37*, 590.
[18] D. M. Huang, M. J. Monteiro, R. G. Gilbert, *Macromolecules* **1998**, *31*, 5175.
[19] J. S. S. Toh, D. M. Huang, P. A. Lovell, R. G. Gilbert, *Polymer* **2001**, *42*, 1915.
[20] S. C. Thickett, R. G. Gilbert, *Polymer* **2004**, *45*, 6993.
[21] J. P. A. Heuts, R. G. Gilbert, I. A. Maxwell, *Macromolecules* **1997**, *30*, 726.
[22] J. P. A. Heuts, G. T. Russell, *Eur. Polym. J.* **2006**, *42*, 3.
[23] H. Gunaydin, S. Salman, N. S. Tuzun, D. Avci, V. Aviyente, *Int. J. Quantum Chem.* **2005**, *103*, 176.
[24] K. Van Cauter, V. Van Speybroeck, P. Vansteenkiste, M. F. Reyniers, M. Waroquier, *ChemPhysChem* **2006**, *7*, 131.
[25] V. Van Speybroeck, K. Van Cauter, B. Coussens, M. Waroquier, *ChemPhysChem* **2005**, *6*, 180.
[26] Gaussian 03, Revision B.03, M. J. Frisch, G. W. Trucks, H. B. Schlegel, G. E. Scuseria, M. A. Robb, J. R. Cheeseman, J. A. Montgomery, Jr., T. Vreven, K. N. Kudin, J. C. Burant, J. M. Millam, S. S. Iyengar, J. Tomasi, V. Barone, B. Mennucci, M. Cossi, G. Scalmani, N. Rega, G. A. Petersson, H. Nakatsuji, M. Hada, M. Ehara, K. Toyota, R. Fukuda, J. Hasegawa, M. Ishida, T. Nakajima, Y. Honda, O. Kitao, H. Nakai, M. Klene, X. Li, J. E. Knox, H. P. Hratchian, J. B. Cross, V. Bakken, C. Adamo, J. Jaramillo, R. Gomperts, R. E. Stratmann, O. Yazyev, A. J. Austin, R. Cammi, C. Pomelli, J. W. Ochterski, P. Y. Ayala, K. Morokuma, G. A. Voth, P. Salvador, J. J. Dannenberg, V. G. Zakrzewski, S. Dapprich, A. D. Daniels, M. C. Strain, O. Farkas, D. K. Malick, A. D. Rabuck, K. Raghavachari, J. B. Foresman, J. V. Ortiz, Q. Cui, A. G. Baboul, S. Clifford, J. Cioslowski, B. B. Stefanov, G. Liu, A. Liashenko, P. Piskorz, I. Komaromi, R. L. Martin, D. J. Fox, T. Keith, M. A. Al-Laham, C. Y. Peng, A. Nanayakkara, M. Challacombe, P. M. W. Gill, B. Johnson, W. Chen, M. W. Wong, C. Gonzalez, and J. A. Pople, Gaussian, Inc., Wallingford CT, **2004**.
[27] A. D. Becke, *Phys. Rev. A* **1988**, *38*, 3098.
[28] a) K. Burke, J. P. Perdew, Y. Wang, *Electronic Density Functional Theory: Recent Progress and New Directions* (Eds.: J. F. Dobson, G. Vignale, M. P. Das), Plenum, New York, **1998**; b) J. P. Perdew, *Electronic Structure of Solids '91* (Eds.: P. Ziesche, H. Eschrig), Akademie, Berlin, **1991**, p. 11; c) J. P. Perdew, J. A. Chevary, S. H. Vosko, K. A. Jackson, M. R. Pederson, D. J. Singh, C. Fiolhais, *Phys. Rev. B* **1992**, *46*, 6671; d) J. P. Perdew, J. A. Chevary, S. H. Vosko, K. A. Jackson, M. R. Pederson, D. J. Singh, C. Fiolhais, *Phys. Rev. B* **1993**, *48*, 4978; e) J. P. Perdew, K. Burke, Y. Wang, *Phys. Rev. B* **1996**, *54*, 16533.
[29] a) C. Lee, W. T. Yang, R. G. Parr, *Phys. Rev. B* **1988**, *37*, 785; b) B. Miehlich, A. Savin, H. Stoll, H. Preuss, *Chem. Phys. Lett.* **1989**, *157*, 200.
[30] A. D. Becke, *J. Chem. Phys.* **1993**, *98*, 5648.
[31] C. Adamo, V. Barone, *J. Chem. Phys.* **1998**, *108*, 664.
[32] a) B. J. Lynch, D. G. Truhlar, *J. Phys. Chem. A* **2001**, *105*, 2936; b) A. P. Scott, L. Radom, *J. Phys. Chem.* **1996**, *100*, 16502.
[33] A detailed definition of the functionals can be found in the Gaussian manual.
[34] B. J. Lynch, P. L. Fast, M. Harris, D. G. Truhlar, *J. Phys. Chem. A* **2000**, *104*, 4811.
[35] A. D. Boese, J. M. L. Martin, *J. Chem. Phys.* **2004**, *121*, 3405.
[36] B. J. Lynch, Y. Zhao, D. G. Truhlar, *J. Phys. Chem. A* **2003**, *107*, 1384.
[37] K. J. Laidler, *Chemical Kinetics*, Harper Collins Publishers, Inc., New York, **1987**.
[38] D. A. McQuarrie, J. D. Simon, *Physical Chemistry—A Molecular Approach*, University Science Books, Sausalito CA, **1997**.
[39] Kinetic database of the National Institute of Standards and Technology http://kinetics.nist.gov/.
[40] a) exp. 1: A. M. Hogg, P. Kebarle, *J. Am. Chem. Soc.* **1964**, *86*, 4558; b) exp. 2: J. A. Kerr, M. J. Parsonage, *Evaluated Kinetic Data on Gas Phase Addition Reactions. Reactions of Atoms and Radicals with Alkenes, Alkynes and Aromatic Compounds*, Butterworths, London, **1972**; c) exp. 3: J. M. Tedder, J. C. Walton, K. D. R. Winton, *J. Chem. Soc. Faraday Trans. 1* **1972**, 1866.

[41] V. Van Speybroeck, D. Van Neck, M. Waroquier, S. Wauters, M. Saeys, G. B. Marin, *J. Phys. Chem. A* **2000**, *104*, 10939.
[42] K. Mitani, T. Ogata, H. Awaya, Y. Tomari, *J. Polym. Sci. Part A* **1975**, *13*, 2813.
[43] O. Vogl, M. F. Qin, A. Zilkha, *Prog. Polym. Sci.* **1999**, *24*, 1481.
[44] W. H. Starnes, Jr., B. J. Wojciechowski, A. Velazquez, G. M. Benedikt, *Macromolecules* **1992**, *25*, 3638.
[45] a) C. W. Wilson, *J. Polym. Sci. Part A* **1963**, *1*, 1305; b) C. W. Wilson, E. R. Santee, Jr., *J. Polym. Sci. Polym. Symp. Ed.* **1965**, *8*, 97.
[46] A. Guyot, *Macromolecules* **1986**, *19*, 1090, and references therein: a) A. Guyot, *Pure Appl. Chem.* **1985**, *57*, 833; b) M.-F. Llauro-Darricades, A. Michel, A. Guyot, H. Waton, R. Petiaud, Q. T. Pham, *J. Macromol. Sci. Chem.* **1986**, *23*, 221.
[47] E. Sidiropoulou, C. Kiparissides, *J. Macromol. Sci. Chem.* **1990**, *27*, 257, and references therein.
[48] T. Moritani, H. Iwasaki, *Macromolecules* **1978**, *11*, 1251.

Received: October 20, 2006
Published online on February 2, 2007

